Supporting Information

Satoh et al. 10.1073/pnas.0912986107

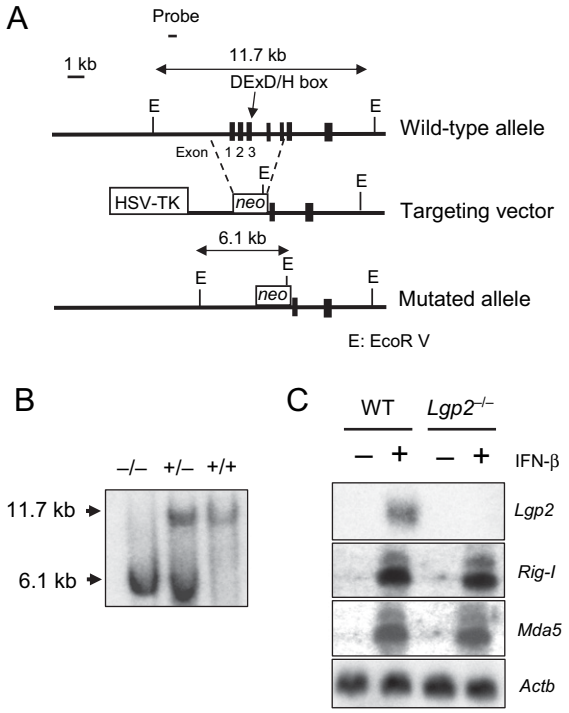

Fig. S1. Targeted disruption of the murine *Lgp2* gene. (*A*) Structures of mouse *Lgp2* gene, targeting vector, and predicted disrupted gene. Closed boxes denote coding exon. E, EcoRV. (*B*) Southern blot analysis of offspring from heterozygote intercrosses. Genomic DNA was extracted from mouse tails, digested with EcoRV, separated by electrophoresis, and hybridized with the radiolabeled probe indicated in (*A*). Southern blotting detects an 11.7-kb band for WT mice ($^{+/+}$), a 6.1-kb band for homozygous mice ($^{-/-}$), and both bands for heterozygous mice ($^{+/-}$). (*C*) Total RNA extracts from WT and *Lgp2*$^{-/-}$ MEFs with or without stimulation by 1000 U/mL IFN-β (Calbiochem) for 8 h were subjected to Northern blot analyses for the expressions of *Lgp2*, *Rig-I*, and *Mda5* mRNAs. The same membranes were rehybridized with an *Actb* probe.

A

	Lgp2$^{+/+}$	*Lgp2*$^{+/-}$	*Lgp2*$^{-/-}$	Total (%)
+/– x +/–	60 (25.4)	155 (65.7)	21 (8.9)	236 (100)
+/– x –/–		361 (77.1)	107 (22.9)	468 (100)

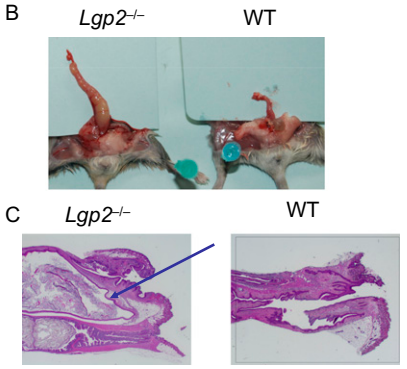

Fig. S2. Developmental defects observed in *Lgp2*$^{-/-}$ mice. (*A*) Genotype analyses of offspring from heterozygote intercrosses or crosses between heterozygotes and homozygotes. (*B*) Enlargement of the uterus observed in *Lgp2*$^{-/-}$ adult female mice. (*C*) Hematoxylin and eosin staining of sagittal sections through the perineum of 12-week-old WT and *Lgp2*$^{-/-}$ mice. Arrow indicates a cystically dilated uterus containing abundant keratin. Sequential sections show that *Lgp2*$^{-/-}$ female mice exhibit vaginal atresia.

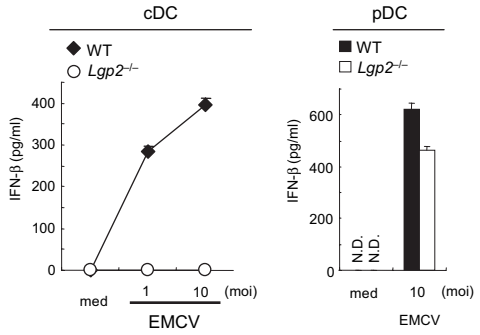

Fig. S3. Role of LGP2 in the recognition of viruses in pDCs and cDCs. B220$^-$CD11c$^+$ cDCs and CD11c$^+$B220$^+$ pDCs were purified from WT and *Lgp2*$^{-/-}$ splenocytes using a FACSAria (BD Biosciences). The cells were then infected with EMCV for 24 h. IFN-β concentrations in culture supernatants were measured by ELISA. N.D., not detected.

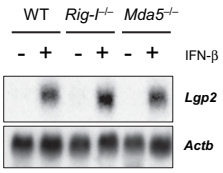

Fig. S4. Normal induction of *Lgp2* in response to IFN-β stimulation in *Rig-I*$^{-/-}$ and *Mda5*$^{-/-}$ MEFs. Total RNA was extracted from WT, *Rig-I*$^{-/-}$, and *Mda5*$^{-/-}$ MEFs cultured with or without 1,000 U/mL IFN-β for 8 h. The expression levels of *Lgp2* mRNA were determined by Northern blot analysis. The same membrane was rehybridized with an *Actb* probe.

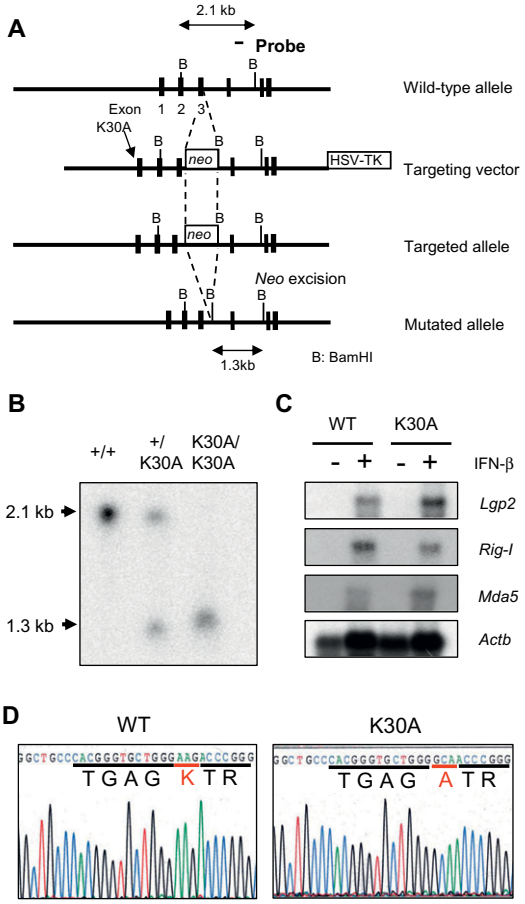

Fig. S5. Generation of mice harboring a K30A point mutation in LGP2. (*A*) Structures of mouse *Lgp2* gene, targeting vector, and predicted disrupted gene. Closed boxes denote coding exon. B, BamHI. (*B*) Southern blot analysis of offspring from heterozygote intercrosses. Genomic DNA was extracted from mouse tails, digested with BamHI, separated by electrophoresis, and hybridized with the radiolabeled probe shown in (*A*). (*C*) Total RNA from WT and Lgp2$^{K30A/K30A}$ MEFs with or without stimulation by 1,000 U/mL IFN-β were subjected to Northern blot analyses for the expressions of *Lgp2*, *Rig-I*, and *Mda5* mRNAs. The same membranes were rehybridized with a *Actb* probe. (*D*) PCR amplification products from WT and *Lgp2*$^{K30A/K30A}$ MEFs were subcloned and sequenced to demonstrate the presence of the K30A mutation. Representative traces are shown.

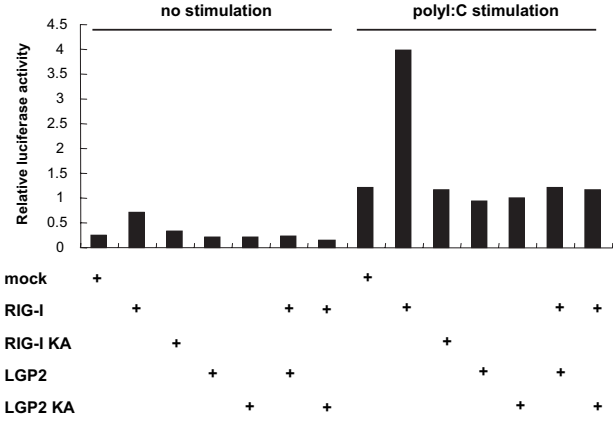

Fig. S6. Inhibition of poly I:C-induced IFN-β promoter activity by overexpression of LGP2 or LGP2 K30A in HEK293 cells. HEK293 cells were transiently transfected with the IFN-β promoter luciferase reporter construct together with the indicated expression plasmids. Cells were stimulated with 1 μg/mL poly I:C for 16 h and then lysed. Cell lysates were analyzed by a luciferase assay.